Structural and magnetic properties of pseudo-two-dimensional triangular antiferromagnets Ba$_3$MSb$_2$O$_9$ (M=Mn, Co, and Ni)

You may also be interested in:

Structural and magnetic properties of pseudo-two-dimensional triangular antiferromagnets $Ba_3MSb_2O_9$ (M = Mn, Co, and Ni)

Yoshihiro Doi[1], Yukio Hinatsu[1] and Kenji Ohoyama[2]

[1] Division of Chemistry, Graduate School of Science, Hokkaido University, Sapporo 060-0810, Japan
[2] Institute for Materials Research, Tohoku University, Sendai 980-8577, Japan

Abstract
The crystal structure and magnetic properties of 6H-perovskites $Ba_3MSb_2O_9$ (M = Mn, Co, and Ni) were investigated. The M = Co and Ni compounds have a hexagonal structure with space group $P6_3/mmc$, while the Mn compound has a monoclinically distorted structure with space group $C2/c$. From the results of magnetic susceptibility and specific heat measurements, it was found that they show an antiferromagnetic transition at 10.0 K (for M = Mn), 3.8 K (Co) and 13.5 K (Ni), and the onset of the magnetic transition was observed much above T_N. The powder neutron diffraction measurements for Mn and Co compounds were carried out, and their magnetic structures were determined. Both compounds adopt the non-collinear 120° structure in the ab-plane. These magnetic properties show the existence of a geometric magnetic frustration derived from the triangular array of magnetic M ions in the ab-plane.

1. Introduction

Geometrically frustrated magnetic materials have attracted a great deal of interest [1, 2]. Most of these systems have a lattice based on a triangular or tetrahedral array of magnetic ions. When there exists an antiferromagnetic interaction between the nearest neighbour ions in such a magnetic lattice, the collinear spin arrangements are no longer in a ground state because it is impossible to satisfy all pairs of nearest neighbours at the same time. Thus, the system is magnetically frustrated. Furthermore, the difference in linkage of such triangles or tetrahedra (edge, corner, and face-sharing) makes the ground state properties very complicated. The two-dimensional triangular lattice consisting of edge-sharing triangles is the simplest example of geometrically frustrated systems; however, they have attracted a great deal of interest since they show anomalous magnetic properties [3] and have the possibility of a resonant valence bond state as proposed by Anderson [4].

We focused our attention on the magnetic properties of 6H-perovskite-type oxides $Ba_3MM'_2O_9$. Their crystal structures can be represented as a framework consisting of the

corner-sharing MO_6 octahedron and the face-sharing M'_2O_9 bi-octahedra. The M ions typically occupy the $2a$ Wyckoff site of space group $P6_3/mmc$, and this site forms the triangular lattice in the *ab*-plane. Hence, if the M ion is magnetic and the M' ion is non-magnetic, they can be seen as a pseudo-two-dimensional triangular magnet, i.e., the layers of magnetic triangular lattice are magnetically separated by the non-magnetic layer containing M'_2O_9. The 6H-perovskites $Ba_3M^{2+}Sb^{5+}_2O_9$ fulfil such a condition. These compounds were first synthesized by Blasse [5]. After that, their structural studies were performed [6–11]. It is found that there exist two structural models with different cation ordering in the octahedral sites: (I) $MO_6 + Sb_2O_9$ for M = Mg, Mn, Co, Ni, and Zn [8–11] and (II) SbO_6+ ordered $MSbO_9$ for M = Ni (prepared at high pressures) [10] and Cu [6, 7, 9]. On the other hand, their magnetic properties were unknown except for the magnetic susceptibility of $Ba_3CoSb_2O_9$ [11, 12], and evidence for long-range magnetic ordering has not been found to date.

In this paper, we will report the magnetic properties of $Ba_3MSb_2O_9$ (M = Mn, Co, and Ni) which adopts the cation arrangement of model (I). In order to elucidate their magnetic properties and check the possibility of the existence of the geometrical frustration, we have performed magnetic susceptibility, specific heat, and neutron diffraction measurements. The specific heat for non-magnetic $Ba_3ZnSb_2O_9$ has also been measured to estimate the magnetic entropy change derived from the magnetic ordering of M ions.

2. Experimental setup

2.1. Sample preparation

Polycrystalline samples of $Ba_3MSb_2O_9$ (M = Mn, Co, Ni, and Zn) were synthesized by the conventional solid-state reaction. As starting materials, $BaCO_3$, MnO_2, CoO, NiO, and ZnO were used. Stoichiometric amounts of them were mixed in an agate mortar. The mixtures were pressed into pellets and then fired in air at 900 °C for 12 h, 1000 °C for 24 h, and 1100 °C for 60 h with several intermediate grindings and pelleting. After that, they were fired at 1100 °C for 24 h (for M = Co) or 1200 °C for 24 h (for M = Mn, Ni and Zn).

2.2. X-ray and neutron diffraction measurements

The x-ray diffraction measurements (XRD) were performed at room temperature in the range $10° \leqslant 2\theta \leqslant 120°$ using a 2θ step size of 0.02° with Cu-K_α radiation on a Rigaku MultiFlex diffractometer. A small amount (<1%) of impurity phase $BaSb_2O_6$ [13] was detected in the x-ray diffraction pattern for all the compounds. For $Ba_3MnSb_2O_9$, the temperature dependence of the XRD patterns was measured between 50 and 250 K using a Rigaku RINT2200 diffractometer. The sample was cooled by a variable temperature cryostat system, CryoMini (Iwatani Industrial Gases Co.).

Powder neutron diffraction profiles were measured for $Ba_3CoSb_2O_9$ (at 2.3 and 10 K) and $Ba_3MnSb_2O_9$ (at 2.3 and 20 K) in the range $3° \leqslant 2\theta \leqslant 153°$ at intervals of 0.1° with a wavelength of 1.82035 Å. Measurements were performed by the Kinken powder diffractometer for high-efficiency and high-resolution measurements, HERMES, of the Institute for Materials Research (IMR), Tohoku University [14], installed at the JRR-3M Reactor in the Japan Atomic Research Institute (JAERI), Tokai. The x-ray and neutron diffraction data were analysed by the Rietveld technique, using the programs RIETAN2000 [15] (for crystal structure) and FULLPROF [16] (for magnetic structure).
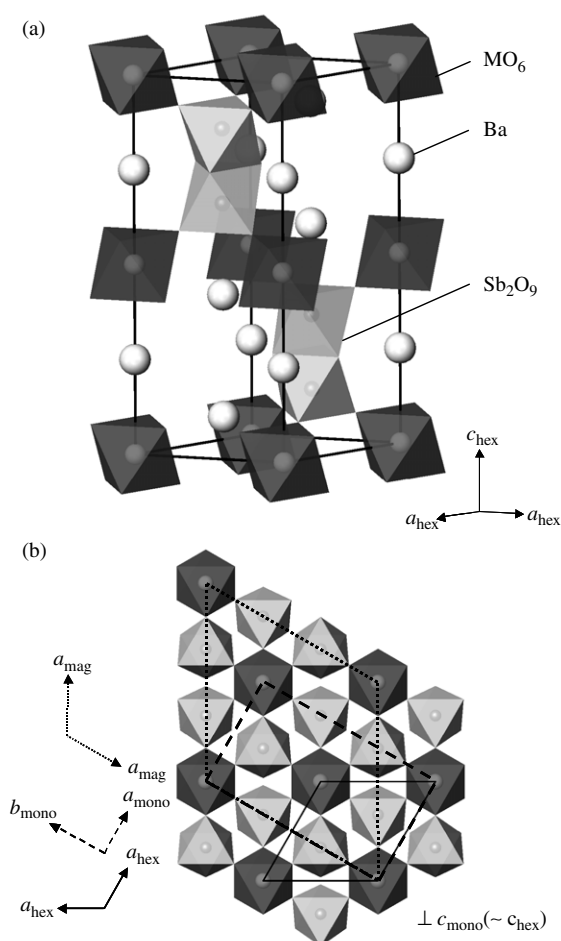
Figure 1. Schematic crystal structure for 6H-perovskite-type oxides $Ba_3MSb_2O_9$ (M = Mn, Co, Ni, and Zn).

2.3. Magnetic and thermal measurements

The temperature dependence of the magnetic susceptibilities was measured under both zero-field-cooled (ZFC) and field-cooled (FC) conditions in an applied field of 0.1 T over the temperature range 1.8–400 K using a SQUID magnetometer (Quantum Design, MPMS-5S).

Specific heat measurements were performed using a relaxation technique with a commercial physical property measurement system (Quantum Design, PPMS model) in the temperature range 1.8–300 K. The sintered sample in the form of a pellet was mounted on a thin alumina plate with grease for better thermal contact.

3. Results and discussion

3.1. Crystal structures

The $Ba_3MSb_2O_9$ (M = Mn, Co, Ni, and Zn) compounds were prepared in the perovskite phase. The x-ray diffraction profiles for M = Co, Ni and Zn were indexed with a hexagonal unit cell, space group $P6_3/mmc$ (no. 194); they adopt the 6H-perovskite structure illustrated in figure 1.

Table 1. Lattice parameters of $Ba_3MSb_2O_9$ determined by XRD at room temperature.

M	a (Å)	c (Å)
Mn[a]	5.9002(1)	14.5815(3)
Co	5.8562(1)	14.4561(3)
Ni	5.8357(2)	14.3956(4)
Zn	5.8571(1)	14.4590(2)

[a] Analysed by the hexagonal model.

Figure 2. Powder neutron diffraction profiles for $Ba_3CoSb_2O_9$ at 10 K (a) and at 2.3 K (b). The upper and lower vertical marks in (a) represent the peak positions for the nuclear reflections of $Ba_3CoSb_2O_9$ and impurity $BaSb_2O_6$, respectively; in (b), those for magnetic reflections are added as bottom vertical marks.

The Rietveld analysis of XRD data show that M and Sb ions occupy the sites in the corner-shared MO_6 octahedron and face-shared M'_2O_9 bi-octahedra, respectively. No evidence of cation disorder was found. The refined lattice parameters are listed in table 1. The lattice parameters are in excellent agreement with those reported by other workers [5, 9–11].

The powder neutron diffraction measurement for $Ba_3CoSb_2O_9$ was performed at 10 K. The result of the Rietveld analysis indicates that $Ba_3CoSb_2O_9$ adopts the 6H-perovskite structure, which is consistent with the results from the XRD data at room temperature. The observed and calculated profiles are shown in figure 2(a). From the previous neutron diffraction experiment, $Ba_3NiSb_2O_9$ is known to keep its hexagonal structure down to 4.2 K [8].

The x-ray diffraction profile for $Ba_3MnSb_2O_9$ (figure 3(a)) can be analysed by the same hexagonal model; however, the diffraction peaks are somewhat broader than those for the
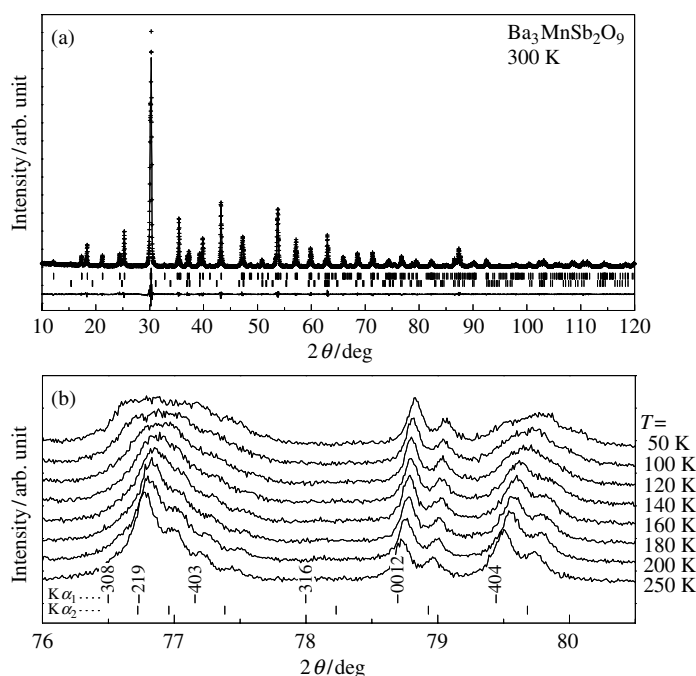
Figure 3. (a) Powder x-ray diffraction profiles for $Ba_3MnSb_2O_9$ at 300 K. (b) Enlarged profiles ($76.0° \leqslant 2\theta \leqslant 80.5°$) measured at 50–250 K. The upper and lower vertical marks in (a) represent the peak positions for the nuclear reflections of $Ba_3CoSb_2O_9$ and impurity $BaSb_2O_6$, respectively.

other compounds. Figure 3(b) shows the temperature dependence of the XRD profiles of $Ba_3MnSb_2O_9$ for $2\theta \sim 78°$. The peak shape of the $\{0\,0\,12\}_{hex}$ reflection (multiplicity $m = 2$) is almost independent of the temperature, while those for the other reflections such as $\{2\,1\,9\}_{hex}$ and $\{4\,0\,4\}_{hex}$ ($m = 24$ and 12, respectively) are obviously broadened with decreasing temperature. This fact indicates that $Ba_3MnSb_2O_9$ has a lower symmetry than the hexagonal one and that this structural distortion becomes larger with decreasing temperature.

In order to determine the crystal structure of $Ba_3MnSb_2O_9$, powder neutron diffraction measurements were performed at 20 K. The observed profile is shown in figure 4(a). Initially, we attempted to fit the data using an orthorhombic model ($a_{hex} \times \sqrt{3}a_{hex} \times c_{hex}$) with space group Cmcm (no 63), which is found in some 6H-perovskite-type compounds [17, 18]; however, the matching between the calculated and observed profiles was unfavourable especially in the high 2θ region (inset graph in figure 4(a)). Finally, it became clear that $Ba_3MnSb_2O_9$ has a monoclinic structure with space group C2/c (no 15). This structure can be represented as a distorted orthorhombic cell with $a_{moco} \sim a_{hex}$, $b_{moco} \sim \sqrt{3}a_{hex}$, $c_{moco} \sim c_{hex}$ and $\beta_{moco} \sim 90.4°$ (figure 1). The structural parameters are summarized in table 2. It has also been confirmed that the type of cation ordering in the M and M' sites is the model (I) ($MnO_6 + Sb_2O_9$). This distorted structure is similar to those for some $Ba_3MM'_2O_9$ compounds with a relatively large M ion, for example, $Ba_3SrRu_2O_9$ [19] and $Ba_3NdRu_2O_9$ [20]. In the $Ba_3MSb_2O_9$ series, the distortion found only in the Mn compound may be explained by the larger size of the Mn^{2+} ion (0.830 Å for high-spin state) compared with other M^{2+} ions (M = Co: 0.745 Å; Ni: 0.690 Å; Zn: 0.740 Å) [21]. From the analysis of neutron diffraction data, neither cation disorder between these two sites nor oxygen defect were found within the experimental error.
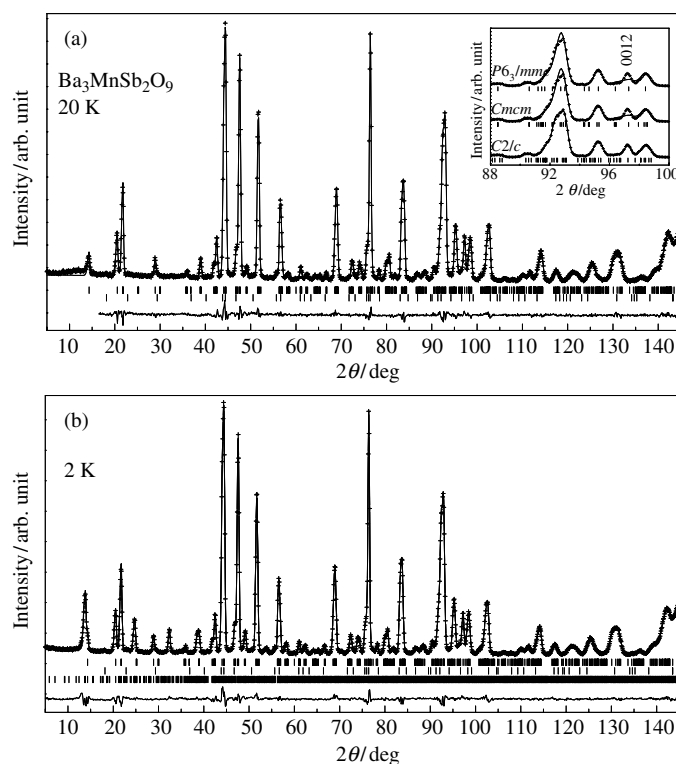
Figure 4. Powder neutron diffraction profiles for $Ba_3MnSb_2O_9$ at 20 K (a) and at 2.3 K (b). The upper and lower vertical marks in (a) represent the peak positions for the nuclear reflections of $Ba_3MnSb_2O_9$ and impurity $BaSb_2O_6$, respectively; in (b), those for magnetic reflections are added as bottom vertical marks. The inset graph in (a) shows calculated profiles using different structural models (see text).

Some bond lengths determined by the x-ray and neutron diffraction measurements are listed in table 3. The XRD data for $Ba_3MnSb_2O_9$ were refined by the hexagonal model because its monoclinic distortion is small at room temperature. The M–O lengths at room temperature for M = Mn, Co, Ni, and Zn are 2.135(5), 2.106(5), 2.091(7), and 2.115(5) Å, respectively. For all the compounds, the shape of the Sb_2O_9 unit is almost the same: the Sb–O(1), Sb–O(2), and Sb–Sb lengths are 2.06–2.09, 1.91–1.94 and 2.83–2.85 Å, respectively. The values of the bond valence sum (BVS) [22] were calculated to be 1.84–2.36 for M ions and 5.02–5.32 for Sb ions, which indicates that their oxidation states are divalent and pentavalent, respectively.

3.2. Magnetic susceptibilities and specific heat

The temperature dependence of the molar magnetic susceptibility (χ_M) for $Ba_3MnSb_2O_9$ is plotted in figure 5. It is found that this compound shows an antiferromagnetic transition at 10.0 K. The ZFC and FC susceptibilities are almost the same over the whole temperature range, and no hysteresis loop was observed from the field dependence of the magnetization below T_N. The magnetic susceptibility in the higher temperature range (100–400 K) was fitted well by the Curie–Weiss law. The magnetic susceptibility shows a deviation from the Curie–Weiss curve below ~50 K. The effective magnetic moment (μ_{eff}) and Weiss constant (Θ) were

Table 2. Structural parameters for $Ba_3MnSb_2O_9$ and $Ba_3CoSb_2O_9$ determined by powder neutron diffraction.

$Ba_3MnSb_2O_9$ at 20 K

Space group $C2/c$ (no. 15), $Z = 4$,
$a = 5.8842(2)$ Å, $b = 10.1863(2)$ Å, $c = 14.5522(2)$ Å, $\beta = 90.428(1)°$

Atom	Site	x	y	z	B (Å^2)
Ba(1)	4e	0	$-0.0011(20)$	1/4	0.12(9)
Ba(2)	8f	0.0053(9)	0.3333(12)	0.0901(2)	0.08(7)
Mn	4a	0	0	0	0.20(10)
Sb	8f	$-0.0079(7)$	0.3338(11)	0.8474(2)	0.10(5)
O(1)	4e	0	0.5160(12)	1/4	0.31(12)
O(2)	8f	0.2796(17)	0.2394(11)	0.2470(4)	0.37(6)
O(3)	8f	0.0092(22)	0.8302(8)	0.0862(7)	0.17(16)
O(4)	8f	0.2684(16)	0.0839(11)	0.0801(4)	0.22(14)
O(5)	8f	0.7543(18)	0.0851(13)	0.0909(5)	0.68(14)

$Ba_3CoSb_2O_9$ at 10 K

Space group $P6_3/mmc$ (no. 194), $Z = 2$,
$a = 5.8413(1)$ Å, $c = 14.4283(2)$ Å

Atom	Site	x	y	z	B (Å^2)
Ba(1)	2b	0	0	1/4	0.07(2)
Ba(2)	4f	1/3	2/3	0.9112(2)	0.10(2)
Co	2a	0	0	0	0.43(9)
Sb	4f	1/3	2/3	0.1518(1)	0.05(4)
O(1)	6h	0.4828(3)	0.9656	1/4	0.37(3)
O(2)	12k	0.1697(3)	0.3394	0.4157(1)	0.30(2)

Table 3. Some selected bond lengths and BVS for $Ba_3MSb_2O_9$.

(a) Hexagonal phase

M	T (K)	M–O(2) (Å)	BVS	Sb–O(1) (Å)	Sb–O(2) (Å)	BVS	Sb–Sb (Å)
Mn[a] (XRD)	300	2.135(5)	2.36	2.093(5)	1.939(5)	5.02	2.844(2)
Co (XRD)	300	2.106(5)	1.96	2.073(5)	1.928(5)	5.22	2.845(2)
Co (ND)	10	2.103(1)	1.98	2.070(2)	1.923(2)	5.28	2.835(3)
Ni (XRD)	300	2.091(7)	1.84	2.071(6)	1.925(7)	5.26	2.849(2)
Zn (XRD)	300	2.115(5)	1.98	2.068(5)	1.920(5)	5.32	2.843(2)

(b) Monoclinic phase

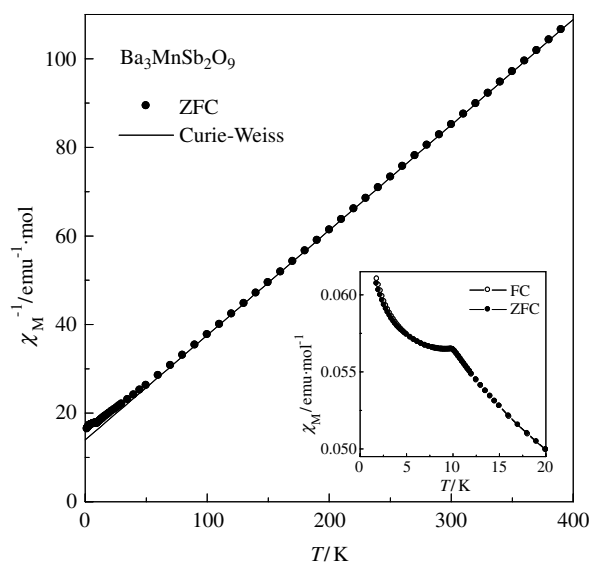| M	T (K)	M–O (Å)	BVS	Sb–O (Å)	BVS	Sb–Sb (Å)
				Sb–O(1) 2.085(5)		
				Sb–O(2) 2.057(8)		
		Mn–O(3) 2.141(9)		Sb–O(2) 2.071(7)		
Mn (ND)	20	Mn–O(4) 2.138(6)	2.32	Sb–O(3) 1.926(9)	5.26	2.825(5)
		Mn–O(5) 2.147(6)		Sb–O(4) 1.943(8)		
				Sb–O(5) 1.908(8)		

[a] Analysed by the hexagonal model.

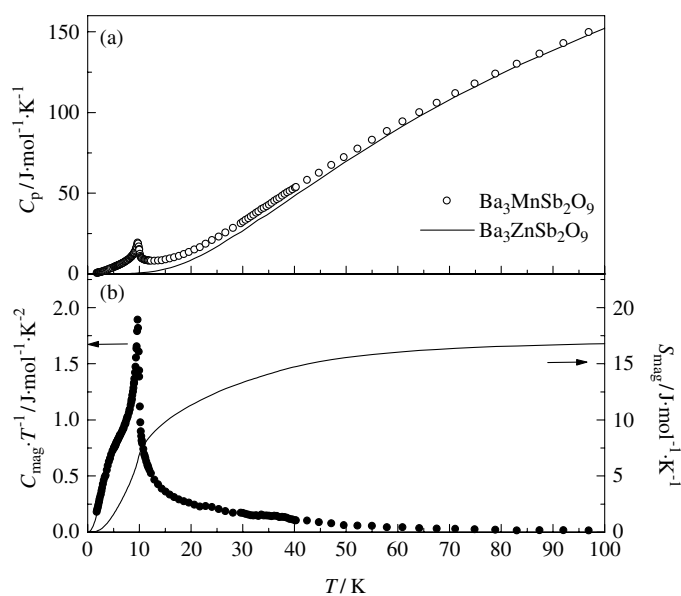**Figure 5.** Temperature dependence of the magnetic susceptibility for Ba$_3$MnSb$_2$O$_9$.

Figure 6. Temperature dependence of (a) the specific heat, (b) magnetic specific heat and magnetic entropy for Ba$_3$MnSb$_2$O$_9$.

found to be 5.83(1)μ_B and $-59.2(5)$ K, respectively. This magnetic moment is in good agreement with the spin-only value of Mn^{2+} (5.92μ_B) calculated from the high-spin state ($S = 5/2$) of a 3d^5 electron configuration. The negative sign of Θ suggests that the dominant magnetic interaction between the Mn^{2+} moments is antiferromagnetic.

The temperature dependence of the specific heat (C_p) for Ba$_3$MnSb$_2$O$_9$ is shown in figure 6(a). A λ-type anomaly is found at 10.0 K, which corresponds with the result of the
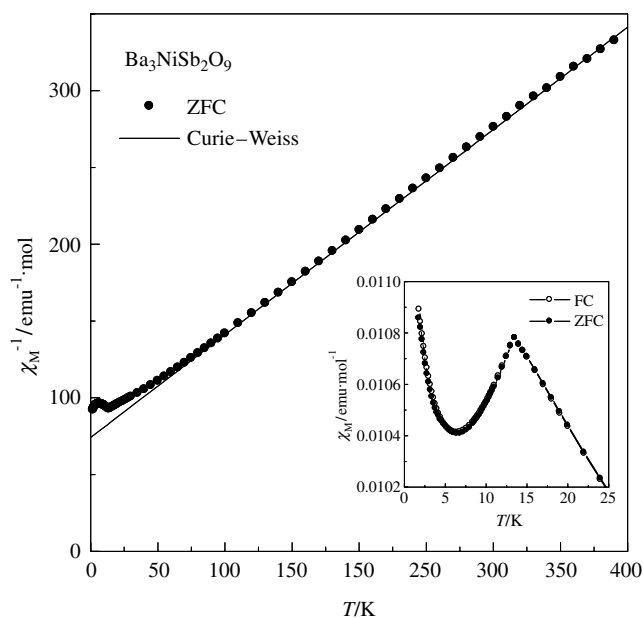
Figure 7. Temperature dependence of the magnetic susceptibility for $Ba_3NiSb_2O_9$.

magnetic susceptibility. In order to estimate the magnetic entropy change (ΔS_{mag}) associated with this magnetic transition, the magnetic specific heat (C_{mag}) was estimated by subtracting the lattice and electronic specific heat from the experimental specific heat of $Ba_3MnSb_2O_9$. For the lattice and electronic contributions, we used the specific heat of the non-magnetic compound $Ba_3ZnSb_2O_9$ whose structure is almost the same as that of $Ba_3MnSb_2O_9$. The temperature dependence of the magnetic specific heat and magnetic entropy is shown in figure 6(b). The magnetic entropy change was 6.9 J mol^{-1} K^{-1} at $T_N = 10.0$ K, and still increases with temperature. Around 50 K, this value reaches $R \ln(2S + 1) = R \ln 6 = 14.9$ J mol^{-1} K^{-1} expected from the magnetic ordering of Mn^{2+} ($S = 5/2$) ions.

The temperature dependences of the magnetic susceptibility and specific heat for $Ba_3NiSb_2O_9$ are shown in figures 7 and 8(a), respectively. An antiferromagnetic transition at 13.5 K is observed from both data. The effective magnetic moment and Weiss constant obtained from the Curie–Weiss fitting to the susceptibility data above 100 K are $3.45(1)\mu_B$ and $-110(2)$ K, respectively. The value of the magnetic moment is typical for the Ni^{2+} ion [23]. The negative Weiss constant indicates the existence of an antiferromagnetic interaction between Ni^{2+} ions. A deviation from the Curie–Weiss curve ($T < \sim 70$ K) is also observed. The magnetic entropy is calculated in the same way as that for the Mn compound and plotted as a function of the temperature in figure 8(b). The magnetic entropy change derived from this transition is 3.6 J mol^{-1} K^{-1} at 13.5 K and it increases with temperature; it is ~ 7.0 J mol^{-1} K^{-1} at 70 K. This value is smaller than $R \ln 3 = 9.13$ J mol^{-1} K^{-1} ($S = 1$); this may be due to the influence of the zero field splitting [24].

Figure 9 shows the temperature dependence of the magnetic susceptibility for $Ba_3CoSb_2O_9$. The Curie–Weiss fitting to the magnetic susceptibility data in the whole temperature range ended in failure because of the bad linearity of χ_M versus T^{-1} at lower temperatures. The Curie–Weiss fitting using a higher temperature data (300–400 K) gives an effective magnetic moment of $5.23(3)\mu_B$ and Weiss temperature of $-51(4)$ K. The value of the
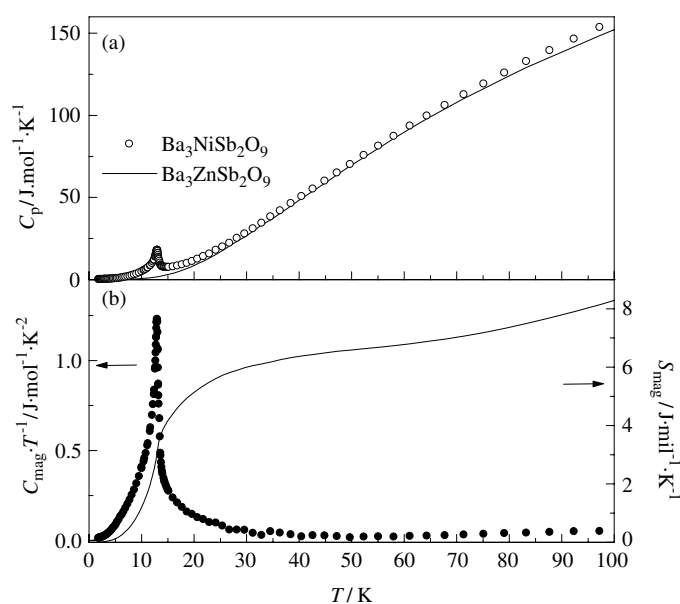
Figure 8. Temperature dependence of (a) the specific heat, (b) magnetic specific heat and magnetic entropy for $Ba_3NiSb_2O_9$.

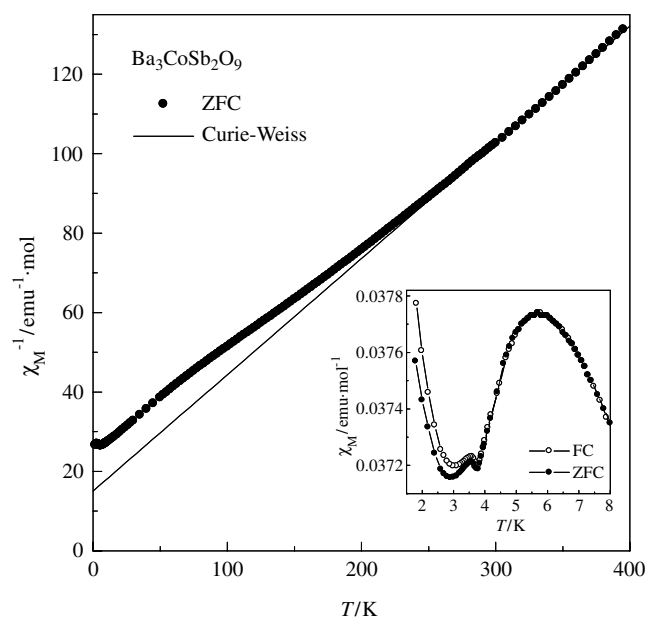**Figure 9.** Temperature dependence of the magnetic susceptibility for $Ba_3CoSb_2O_9$. The inset shows the detailed susceptibility at low temperatures.

magnetic moment is reasonable for the Co^{2+} ion in the high-spin state with a contribution from the orbital angular momentum [23]. At lower temperatures, a broad maximum (6.0 K) and a sharp cusp (3.8 K) are found. The temperature dependence of the specific heat is plotted in figure 10(a), which shows a λ-type anomaly at 3.8 K. Thus, long-range antiferromagnetic
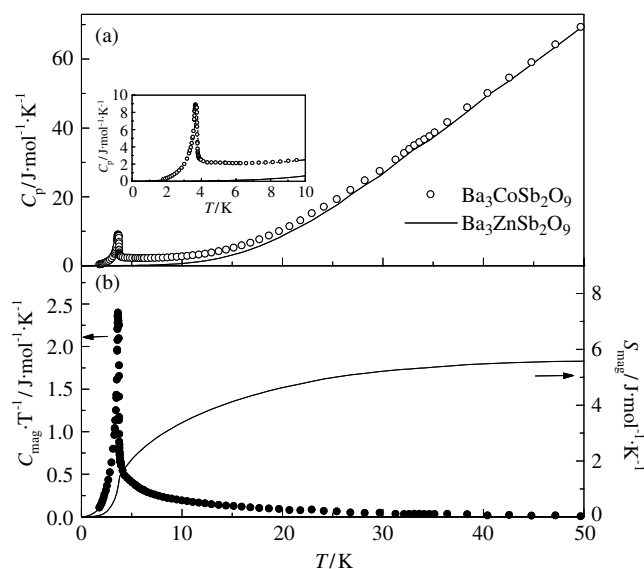
Figure 10. Temperature dependence of (a) the specific heat, (b) magnetic specific heat and magnetic entropy for $Ba_3CoSb_2O_9$.

ordering of Co^{2+} moments occurs at this temperature. The calculated magnetic entropy is plotted as a function of temperature in figure 10(b). The magnetic entropy change is $1.5\,J\,mol^{-1}\,K^{-1}$ at T_N; however, it increases with temperature and reaches $5.5\,J\,mol^{-1}\,K^{-1}$ at 40 K. This indicates that the Co^{2+} ion has a doublet ground state ($\Delta S_{mag} = R\ln 2 = 5.76\,J\,mol^{-1}\,K^{-1}$).

From the results of magnetic susceptibility and specific heat measurements, it has been found that the $Ba_3MSb_2O_9$ (M = Mn, Co, and Ni) compounds show some characteristic magnetic properties: an antiferromagnetic transition at low temperatures, large negative Weiss constants ($|\Theta|/T_N = 5.9$–13.4), and a broad maximum in the magnetic susceptibility versus temperature curve (for the Co compound only). In addition, the decrease in the magnetic entropy with a decrease in temperature and the deviation of magnetic susceptibility from the Curie–Weiss law were observed at temperatures much higher than T_N. These features may reflect their two-dimensional character. The magnetic frustration in the *ab*-plane containing the triangular array of the magnetic ions would make long-range magnetic ordering difficult.

At sufficiently low temperatures, it was found that the $Ba_3MSb_2O_9$ (M = Mn, Co and Ni) compounds show a magnetic transition. The existence of the magnetic frustration may affect the spin arrangement of M^{2+} ions. Therefore, in order to determine their magnetic structures, we performed powder neutron diffraction measurements below T_N for $Ba_3CoSb_2O_9$ and $Ba_3MnSb_2O_9$.

3.3. Magnetic structures

The neutron diffraction profile for $Ba_3CoSb_2O_9$ at 2.3 K is shown in figure 2(b). Some additional reflection peaks were found at lower angles, which were not observed at 10 K. They are associated with the magnetic ordering of Co^{2+} moments and indexed in the crystallographic unit cell with $h = n_1 \pm 1/3$, $k = n_2 \pm 1/3$, and $l = 2n_3 + 1$ (n_i: integer). In order to determine the magnetic structure, we used a magnetic unit cell of $\sqrt{3}a_{hex} \times \sqrt{3}a_{hex} \times c_{hex}$ (see figure 1(b))

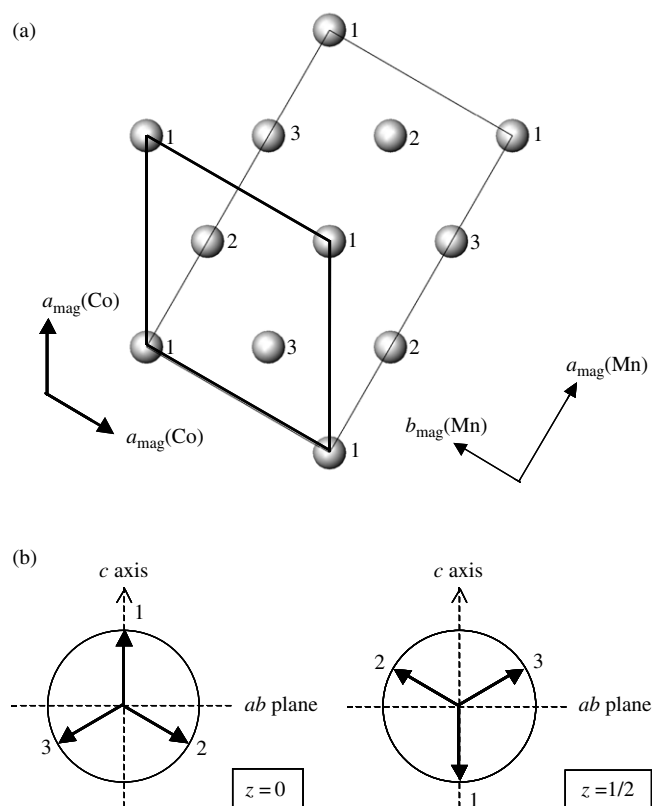**Figure 11.** Magnetic structures of $Ba_3CoSb_2O_9$ and $Ba_3MnSb_2O_9$: (a) magnetic unit cell in *ab*-plane (diamagnetic ions are omitted) and (b) direction of the magnetic moments of Co^{2+}. In the case of $Ba_3MnSb_2O_9$, all the magnetic moments of Mn^{2+} are lying in the *ab*-plane and form the same 120° structure.

in which the Co sublattice is divided into six sublattices: (0,0,0), (1/3,2/3,0), (2/3,1/3,0), (0,0,1/2), (1/3,2/3,1/2), and (2/3,1/3,1/2). The value of l is odd for all the magnetic reflections, thus we assumed that the magnetic moment of the Co ion at $(x, y, 0)$ is antiparallel to that at $(x, y, 1/2)$. As a result of the Rietveld analysis, it was found that $Ba_3CoSb_2O_9$ adopts a so-called 120° structure. This magnetic structure is illustrated in figure 11. The magnetic moments from three sublattices lie in a common plane with an inclination of 120° to each other. The best fit was obtained when the direction of the magnetic moment of one sublattice was parallel to the *c*-axis.

For $Ba_3MnSb_2O_9$, the neutron diffraction profile measured at 2.3 K is shown in figure 4(b). Magnetic reflection peaks were observed in the low angle region and indexed in the crystallographic unit cell with $h = n_1 \pm 1/3$, $k = n_2$, and $l = 2n_3 + 1$ (n_i: integer). They were analysed by the Rietveld method using a magnetic unit cell ($\sqrt{3}a_{mono} \times b_{mono} \times c_{mono}$). As a result of this analysis, it has been found that these magnetic reflections can be explained by the same 120° structure. All the magnetic moments of Mn^{2+} are lying in the *ab*-plane.

The magnetic structures determined for these compounds have been often observed in the Heisenberg antiferromagnets with a magnetic triangular lattice [3, 25, 26]. The difference in the magnetic structures between $Ba_3CoSb_2O_9$ and $Ba_3MnSb_2O_9$ is whether the spin triangle is

confined in a plane containing the c axis or the ab plane. This result may be attributed to the difference in the single-ion anisotropy which affects the direction of the spin triangle [3]. The Co^{2+} and Mn^{2+} ions in these compounds have the Ising and XY characters to some extent, respectively. The ordered magnetic moments for the Co^{2+} and Mn^{2+} ions were determined to be $1.35(4)\mu_B$ and $4.08(2)\mu_B$, respectively. These values are smaller than those expected from the high-spin $3d^7$ ($3\mu_B$) and $3d^5$ ($5\mu_B$) electronic configurations, respectively. This result may be due to the magnetic frustration and thermal fluctuation.

Acknowledgments

References

[1] Greedan J E 2001 *J. Mater. Chem.* **11** 37–53
[2] Ramirez A P 1994 *Annu. Rev. Mater. Sci.* **24** 453–80
[3] Collins M F and Petrenko O A 1997 *Can. J. Phys.* **75** 605–55
[4] Anderson P W 1973 *Mater. Res. Bull.* **8** 153–60
[5] Blasse G 1965 *J. Inorg. Nucl. Chem.* **27** 993–1003
[6] Köhl V P and Reinen D 1977 *Z. Anorg. Allg. Chem.* **433** 81–93
[7] Köhl V P 1978 *Z. Anorg. Allg. Chem.* **442** 280–88
[8] Jacobson A J and Calvert A J 1978 *J. Inorg. Nucl. Chem.* **40** 447–9
[9] Treiber V U and Kemmler-Sack S 1982 *Z. Anorg. Allg. Chem.* **487** 161–77
[10] Battle P D, Jones C W, Lightfoot P and Strange R 1990 *J. Solid State Chem.* **85** 144–50
[11] Istomin S Ya, Koutcenko V A, Antipov E V, Lindberg F and Svensson G 2004 *Mater. Res. Bull.* **39** 1013–22
[12] Battle P D, Gore J G, Hollyman R C and Powell A V 1995 *J. Alloys Compounds* **218** 110–6
[13] DeBoer B G, Young R A and Sakthivel A 1994 *Acta Crystallogr.* C **50** 476–82
[14] Ohoyama K, Kanouchi T, Nemoto K, Ohashi M, Kajitani T and Yamaguchi Y 1998 *Japan. J. Appl. Phys.* **37** 3319–26
[15] Izumi F and Ikeda T 2000 *Mater. Sci. Forum* **321–324** 198–203
[16] Rodrigues-Carvajal J 1993 *Physica* B **192** 55–69
[17] Lightfoot P and Battle P D 1990 *J. Solid State Chem.* **89** 174–83
[18] Rijssenbeek J T, Huang Q, Erwin R W, Zandbergen H W and Cava R J 1999 *J. Solid State Chem.* **146** 65–72
[19] Zandbergen H W and IJdo D J W 1984 *Acta Crystallogr.* C **40** 919–22
[20] Doi Y, Hinatsu Y, Shimojo Y and Ishii Y 2001 *J. Solid State Chem.* **161** 113–20
[21] Shannon R D 1976 *Acta Crystallogr.* A **32** 751–67
[22] Brown I D and Altermatt A 1985 *Acta Crystallogr.* B **41** 244–7
[23] Carlin R L 1986 *Magnetochemistry* (Berlin: Springer) ch 4
[24] Abragam A and Bleaney B 1986 *Electron Paramagnetic Resonance of Transition Ions* (New York: Dover)
[25] Fruchart D, Bertaut E F, Madar R, Lorthioir G and Fruchart R 1971 *Solid State Commun.* **9** 1793–7
[26] Sunaga T, Tanaka M, Sakai N and Tsunoda Y 2001 *J. Phys. Soc. Japan* **70** 3713–8